A Ray Tracer for optimizing solar concentrating systems: The case of discretized Compound Parabolic Concentrator

Casiana Blasius Lwiwa [a,*], Ole Jørgen Nydal [a]

[a] *Norwegian University of Science and Technology, 7491, Trondheim, Norway*
casiana.b.lwiwa@ntnu.no

Abstract

Concentrating solar systems use reflective surfaces to concentrate sunlight onto a small area, where it is absorbed and converted to heat. Many classes of concentrating collectors such as Compound Parabolic Concentrators (CPCs), parabolic dish and parabolic trough are available, each with different concentrating ratio and maximum absorber temperature, depending on the type of applications. A simplified 3D Compound Parabolic Concentrator (CPC) with 2 rings and 4 sectors has been designed. The designed CPC is cost effective as it requires only 8 mirrors to cover the reflector surface. It does not require sun tracking, but have capability to accept incoming solar radiation over a relatively wide range of angles. For further capturing of the solar radiations, tilting of the CPC during a day can be made a few times. This study aims to model the discretized 3D CPC using the ray tracing, to optimize the CPC for achieving optimal interceptions on a 0.2 m diameter cylindrical absorber, placed inside the CPC. The ray tracing methodology is presented together with the results of the interceptions on the cylindrical absorber using the discretized CPC. Results show the effect of tilting the discretized CPC is not very strong as the interception values are slightly reduced and the curves a little bit not symmetric around the normal sun angles.

1. Introduction

The concentrating solar thermal systems use mirrors or lenses to concentrate and collect solar radiations onto an absorber in order to produce high temperatures needed for various applications. Compound Parabolic Concentrators (CPC) falls under the class of non imaging concentrators which can be promising options for thermal solar energy applications. The important features of the CPC is that it does not require tracking of the sun and the capability of collecting solar radiations over a wide range of angles [1]. The general principles of a CPC are reported in [1, 2].

CPC is made up of two parabolic mirror segments with closely located focal points and their axes inclined to each other, such that rays incident within the acceptance angle of the CPC are collected at the lower exit opening. Fig. 1 gives the schematic diagram of the 2D CPC.

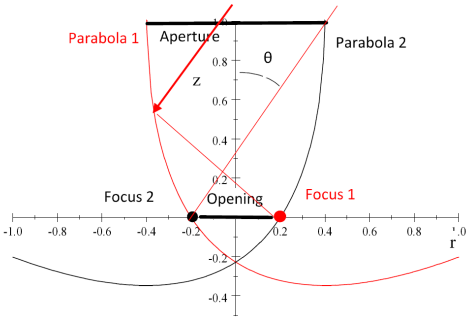

Figure 1: The schematic diagram of the 2D CPC

The 2D CPC can have an ideal performance where all incoming rays within the acceptance angle will pass through the lower opening. The concentration ratio for a 2D CPC is given by [1, 3]:

$$C = \frac{A_{ap}}{A_{ab}} = \frac{1}{sin\theta} \tag{1}$$

where; C is the concentration ratio, A_{ap} is the aperture area, A_{ab} is the absorber area and θ is the acceptance half angle.

The CPC equation can be obtained from the rotation and shift of parabolas. Let a coordinate system in the focus point of a parabola be (z, r). (Z, R) is the rotated coordinate system, where the rotation is around the focal point and where the parabola has been shifted distance a. Then, the parabola with focal point in the origo is given by:

$$z = \frac{r^2}{4f} - f \tag{2}$$

To represent both parabolas in one coordinate system, denoted (R, Z), a rotation and translation is made. The rotation angle is ϕ and the displacement along the R axis is a as shown in Eqs. 3-8.

Rotation

$$r = Rcos(\phi) + Zsin(\phi) \tag{3}$$

$$z = -Rsin(\phi) + Zcos(\phi) \tag{4}$$

For compact notation, we define:

$$s = sin(\phi) \tag{5}$$

$$c = cos(\phi) \tag{6}$$

$$r = Rc + Zs \tag{7}$$

$$z = -Rs + Zc \tag{8}$$

The inverted transformations are:

$$R = cr - sz \tag{9}$$

$$Z = cz + rs \tag{10}$$

Inserting into the equation for the parabola in Eq. 2, for the rotation gives:

$$-Rs + Zs = \frac{(Rs + Zs)^2}{4f} - f \tag{11}$$

Solving for Z, we obtain two solutions:

$$Z_1 = \frac{1}{s^2}\left(2f\sqrt{\frac{1}{f}(f - Rs)(c^2 + s^2)} + 2cf - Rcs\right) \tag{12}$$

$$Z_2 = -\frac{1}{s^2}\left(2f\sqrt{\frac{1}{f}(f - Rs)(c^2 + s^2)} - 2cf + Rcs\right) \tag{13}$$

The solutions for Z_1 and Z_2 are shown on Fig. 2. Inspection shows that of the two solutions, Z_2 is the relevant for the CPC (black curve in the figure).

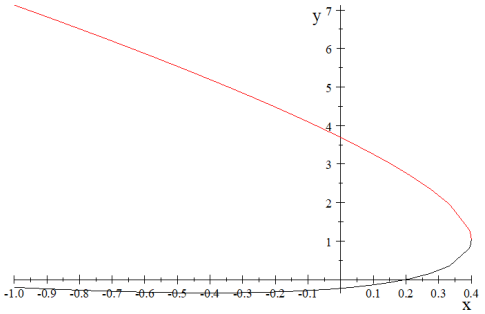

Figure 2: The schematic diagram of the CPC from rotating the parabolas

CPC can be generated by rotating positive and shifting left which gives the right side of the CPC and mirror on the other side gives the left side of the CPC. For a 3D CPC, we consider the right side and revolve around z axis. Considering only the rotation, where the origo is the focal point for both, we obtain Fig. 3.

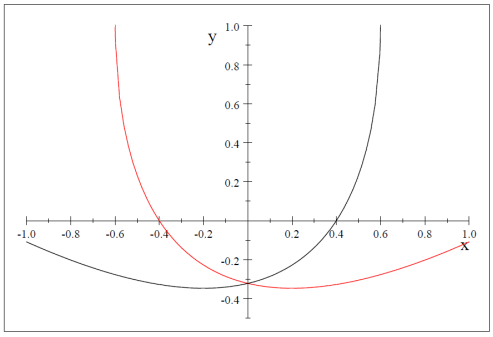

Figure 3: The schematic diagram of the CPC from rotating the parabolas; the origo is the focal point for both parabolas

The parabola should be shifted such that the focal point is at the rim of the other. The black will then be shifted to the left such that the focal point (now at the origo) reaches the red curve. By symmetry this should be the solution to $Z = 0$. We call this shift b. In the figure it is $b = 0.4$. But as we keep the origo, we shift the other way with a similar amount. So, we can only shift half the distance given by the $Z = 0$ solution. The real shift is what enters the CPC equation, with the variable a. So, b can be obtained from $Z = 0$ solution and then $a = \frac{b}{2}$.

The solution for the only rotated, $Z_2 = 0$ is given by:

$$0 = -\frac{1}{s^2}\left(2f\sqrt{\frac{1}{f}(f - Rs)} - 2cf + Rcs\right) \tag{14}$$

The solutions for the shift b becomes:

$$b = -\frac{2f}{c^2 s}\left(\sqrt{-c^2 + 1} - c^2 + 1\right) \tag{15}$$

$$b = \frac{2f}{c^2 s}\left(\sqrt{-c^2 + 1} + c^2 - 1\right) \tag{16}$$

As c is less than one, the first solution is the one on the negative side. We are looking for the other from Eq. 16.

Simplifying we get:

$$f = \frac{b}{2}(1 + s) = a(1 + s) \tag{17}$$

a is now half the lower opening

Thus, the CPC equation becomes:

$$Z = -\frac{1}{s^2}\left(\sqrt{A + BR} + C - csR\right) \tag{18}$$

where;
$A = a^2(s + 1)$
$B = -as(s - 1)$
$C = -ac(2 - s)$

The amount of solar radiations intercepted by the CPC is directly related to the width of the entrance aperture and the acceptance angle [4], where the aperture allows the concentration of the solar radiation at the absorber. The direction and angle of the solar irradiation can be obtained by using the geometrical coordinates and time which works as a seasonally altered clock.

The aperture size of the absorber affects ray interceptions with the absorber such that, the larger the aperture size, the higher the interceptions on the absorber. Interception ratio is the ratio of the sun rays hitting the reflector and reflecting on the absorber. It shows the performance of a solar concentrator to enable the determination of the optical losses. Interception ratio depends on the geometry of the optical systems and the sun angles, the solar tracking errors and varies for smooth and tiled surfaces [5, 6].

Fig. 4 is a setup of the discretized CPC, a cylindrical absorber and the vertical sun. The designed CPC is strongly simplified but cost effective since only 8 mirrors are needed to cover the reflector surface.

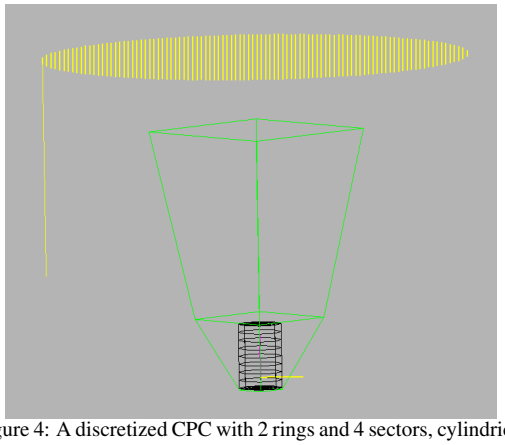

Figure 4: A discretized CPC with 2 rings and 4 sectors, cylindrical absorber and vertical sun

2. Ray tracing methodology

Ray tracing technique is used for the optical analysis of the solar concentrating systems. It encompasses the tracing of the individual paths of a large number of incident solar rays passing through the optical systems to determine the distribution pattern on the surface of interest. For analysis of thermal systems, ray tracing can give the distribution and intensities at the absorber [5].

Various software are available for ray tracing [7]. An in-house ray tracer algorithm (Tracelt) is implemented in C++ with Qt and the Open GL [5]. The Qt library provides the basis for the user interface, and the OpenGL library for the 3D graphical visualization. A model view of the data is included, where panels can be selected for translation, rotation or deletion. A screen capture of the program is shown in Fig. 5.

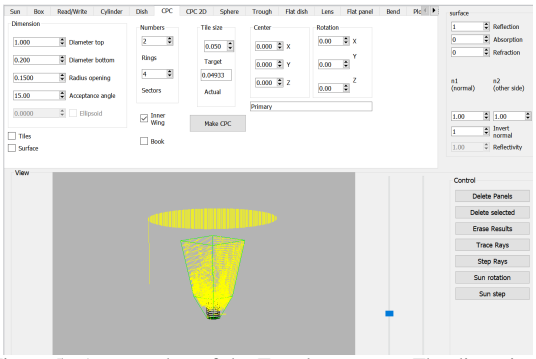

Figure 5: A screenshot of the Tracelt program: The discretized CPC, cylindrical absorber and the vertical sun

Panels are the basic elements in Tracelt, and they can be absorbers, reflectors or refractors. An array of sun rays (origin and direction) of individual rays are made. For each ray, rays intersection with the panels are computed. Ray tracing is performed after the reflections and absorptions system are made. For the nearest intersection, if the reflection side of the panel, the reflected rays (origin and direction) are made and repeated (recursive function), otherwise, the rays are terminated (absorber or backside).

In this study, the reflectivity is assumed to be 100%, mirror impections are ignored. A high density of sun rays leads to longer computation times (minutes). In the current case, a sun grid size of 2 cm can be sufficient to give low simulation times and acceptable number of rays for the visualization. The rays can be visualized as lines, points or as colors on the surfaces. Computational loops with varying sun angles or geometrical parameters have been included.

After the ray tracing is completed, the data generated by the Tracelt are saved in a text file and can be re initiated afterwards. The data can be post processed with other software. In our case, MATLAB was used for better graphical presentations as compared to what is implemented in Tracelt program. Fig. 6 shows the flow chart for the description of the ray tracer algorithm.

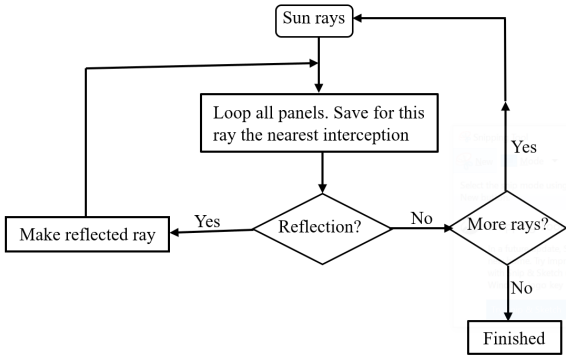

Figure 6: Flow chart of the ray tracer algorithm for simulating the performance of solar concentrating systems

3. Ray tracing sequence

The basic equation encountered in a ray tracer is to determine the intersections between a line and a surface. Subsequently, the reflected ray from the incoming ray and the surface normal vector at the intersection point are computed. Consider a ray, with point of intersection at P (x, y, z) such that:

$$\vec{P} = \vec{S} + u\vec{d} \tag{19}$$

$u\vec{d}$ is a line that intersects $\vec{P}$ and $\vec{d}$ is a unit vector.

A surface, can be cylinder, sphere, flat plate etc. and can be described by an algebraic relation. For a CPC, this relation is given in Eq. 18.

Assuming the starting point of the sun to be S(s_x, s_y, s_z). The components of parametric equation for each ray can be described by:

$$\begin{cases} x = s_x + u \cdot d_x \\ y = s_y + u \cdot d_y \\ z = s_z + u \cdot d_z \end{cases} \tag{20}$$

where (s_x, s_y, s_z) are initial points and (d_x, d_y, d_z) are the direction vector.

Inserting the P components of Eq. 20 into the shape of the surface f(x, y, z) = 0 gives an equation for u and thus the intersection point, f(u)=0.

To formulate reflections in a ray tracing technique, the normal vector ($\vec{n}$), calculated at the point of intersection (P), has the reflected ray and direction ($\vec{d}$) given by:

$$\vec{r} = \vec{d} - 2(\vec{d} \cdot \vec{n})\vec{n} \tag{21}$$

For a 2D CPC, the solution for u can be solved analytically, but for a 3D CPC, the solution for u can be obtained using numerical methods such as bisect iteration scheme [8].

4. Examples of ray tracing for analysis of solar concentrators

Studies with Tracelt include references [4, 5, 9, 10] as briefly described below:

4.1. Optimization of the size of surface tile on a CPC

Tracelt was used to perform a sensitivity analysis on the dimensions of mirror tiles on the CPC surface. The results show that uniform tile sizes up to 15 cm gives quite similar interception ratios (less than 10% changes) compared with the smooth surface. Larger and non-uniform tiles discretized in terms of rings and sectors can give similar results [4].

4.2. Simulation of a light guide efficiency

The tracelt has been applied for evaluation of a light guide to provide the energy transfer from a solar concentrator to an absorber. Using a tracelt ray tracer, results shows energy losses through a light guide can be associated with the number of internal reflections in the guide, and the number of back scattered rays through the tube inlet [9].

4.3. Double reflector system

The optical performance of the double reflector system was investigated by means of a ray tracer. Results shows that increasing the absorber dish from 0.1 to 0.2 m makes the system more tolerant for tracking accuracy and for low solar angles. A large absorber dish also reduces the risk of superheating the top plate which has conduction based heat transfer to a salt storage [5].

4.4. Evaluation of the SK14 solar concentrator as a solar fryer

SK14 is a solar dish reflector which is made for cooking in a pot positioned at the focal point. [10] used Tracelt ray tracing to evaluate the SK14 solar concentrator to fry Ethiopian injera bread. Ray tracing reveals that the reflected rays spread more evenly on the pan, but also gives higher losses compared with an ideally smooth reflector.

The novelty of this study is to analyze the efficiency of this simplified system where the intention is to accumulate heat for cooking on the cylindrical absorber.

5. Simulation parameters

A simplified CPC (15 degrees acceptance angle) with 2 rings and 4 sectors has been applied in the simulations. The surface of the reflector is covered with 8 mirrors. The CPC has aperture diameter of 1.0 m and exit diameter opening of 0.15 m. The cylindrical absorber has 20 cm diameter and 30 cm length.

6. Results

The sun angle-interception values were compared for the fixed and tilted CPC at 5, 10 and 15 degrees. Fig. 7 shows the effects of tilting the discretized CPC as compared to the fixed CPC. In all cases, the absorber is fixed. The sun angles are choosen to exceed the maximum acceptance angle (15 degrees) to see the effect of using the discretized CPC beyond the design regions. The effect of tilting the discretized CPC does not affect much the interception values, as they are slightly reduced and the curves a little bit not symmetric around the normal sun angles.

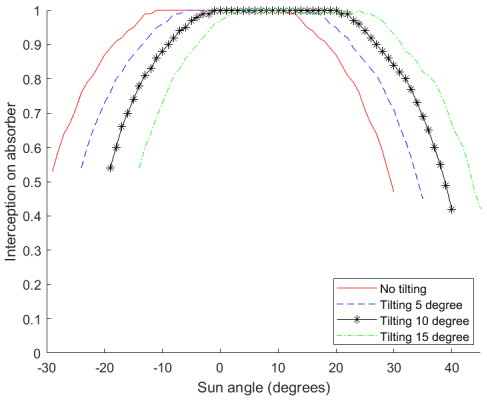

Figure 7: Effects of tilting the discretized 3D CPC to the interceptions on the absorber

7. Summary and Discussions

The ray tracing methodology for optimizing the solar concentrating systems have been presented, together with the results of the interceptions on the cylindrical absorber using the discretized CPC. Results shows when the CPC is tilted while the absorber is kept stationary, the interception values are slightly reduced and the curves somewhat not symmetric around the normal sun angles.

The CPC can be built with 8 mirrors and still give high interceptions on the absorber.

Acknowledgment

The authors extend their gratitude to the Norwegian University of Science and Technology, NTNU Energy strategic Area for financial support to the study.

References

[1] A. Rabl, "Comparison of solar concentrators," *Solar energy*, vol. 18, no. 2, pp. 93–111, 1976.

[2] R. Winston and H. Hinterberger, "Principles of cylindrical concentrators for solar energy," *Solar Energy*, vol. 17, no. 4, pp. 255–258, 1975.

[3] A. Rabl, "Optical and thermal properties of compound parabolic concentrators," *Solar energy*, vol. 18, no. 6, pp. 497–511, 1976.

[4] C. Lwiwa and O. Nydal, "3d ray tracing for optimizing the size of surface tiles on a compound parabolic concentrator," Southern African Sustainable Energy Conference, South Africa, 17-19 November, 2021., 2022.

[5] O. J. Nydal, "Ray tracing for optimization of a double reflector system for direct illumination of a heat storage," *Energy Procedia*, vol. 57, pp. 2211–2220, 2014.

[6] K. Nyeinga, D. Okello, and O. J. Nydal, "A ray tracer model for analysis of solar concentrating systems," *Journal of Energy in Southern Africa*, vol. 30, no. 1, pp. 8–20, 2019.

[7] D. Jafrancesco, J. P. Cardoso, A. Mutuberria, E. Leonardi, I. Les, P. Sansoni, F. Francini, and D. Fontani, "Optical simulation of a central receiver system: Comparison of different software tools," *Renewable and Sustainable Energy Reviews*, vol. 94, pp. 792–803, 2018.

[8] G.-L. Dai, X.-L. Xia, C. Sun, and H.-C. Zhang, "Numerical investigation of the solar concentrating characteristics of 3d cpc and cpc-dc," *Solar Energy*, vol. 85, no. 11, pp. 2833–2842, 2011.

[9] O. Nydal, "Ray tracing for simulation of a light guide efficiency," 3rd Southern African Solar Energy Conference, South Africa, 11-13 May, 2015., 2015.

[10] O. J. Nydal and A. Tesfay, "Ray tracing for evaluation of the sk14 solar concentrator as a solar fryer," in *Conference Proceedings, ISES Solar World Congress, Daegu, Korea, 8–12 November 2015*, 2015.